A Novel Energy Management Strategy in Electric Vehicle Based on H Self-gain Scheduled for Linear Parameter Varying Systems

Sellali, Mehdi; Betka, Achour; Djerdir, Abdesslem; Yang, Y.; Bahri, Imene; Drid, Said

Published in:
IEEE Transactions on Energy Conversion

DOI (link to publication from Publisher):
10.1109/TEC.2020.3017811

Publication date:
2020

Document Version
Accepted author manuscript, peer reviewed version

This article has been accepted for publication in a future issue of this journal, but has not been fully edited. Content may change prior to final publication. Citation information: DOI 10.1109/TEC.2020.3017811, IEEE Transactions on Energy Conversion

A Novel Energy Management Strategy in Electric Vehicle Based on H∞ Self-gain Scheduled for Linear Parameter Varying Systems

Mehdi Sellali, Student Member, IEEE, Achour Betka, Abdesslem Djerdir, Yongheng Yang, Senior Member, IEEE, Imene Bahri and Said Drid, Senior Member, IEEE.

Abstract— The present paper exhibits a real time assessment of a robust Energy Management Strategy (EMS) for battery-super capacitor (SC) Hybrid Energy Storage System (HESS). The proposed algorithm, dedicated to an electric vehicular application, is based on a self-gain scheduled controller, which guarantees the H∞ performance for a class of linear parameter varying (LPV) systems. Assuming that the duty cycle of the involved DC-DC converters are considered as the variable parameters, that can be captured in real time, and forwarded to the controller to ensure both; the performance and robustness of the closed-loop system. The subsequent controller is therefore time-varying and it is automatically scheduled according to each parameter variation. This algorithm has been validated through experimental results provided by a tailor-made test bench including both the HESS and the vehicle traction emulation system. The experimental results demonstrate the overall stability of the system, where the proposed LPV supervisor successfully accomplishes a power frequency splitting in an adequate way, respecting the dynamic of the sources. The proposed solution provides significant performances for different speed levels.

Keywords — Gain scheduled, H∞, Linear parameter varying (LPV), Battery, Super capacitor.

NOMENCLATURE

V_{Batt} : Battery voltage (V).
V_0 : Open circuit voltage (V).
I_{Batt} : Battery current (A).
I_{Batt_ref} : Battery reference current (A).
R_{Batt} : Internal battery resistance (Ω.)
SOC : State of charge (%).
Q :Current amount (Ah).
V_{SC} : Super-capacitor voltage (V).
V_{SCref} : Super-capacitor reference voltage (V).
ERS : Equivalent Serial Resistance (Ω).
C_{SC} : Supercapacitor capacitor (F).
I_{SC} : Super capacitor current (A).
I_{SCref} : Super capacitor reference current (A).
I_{load} : Load current (A).
V_{DC} :DC-link voltage (V).
V_{DCref} :DC-link reference voltage (V).
C_{DC} : DC-link capacitor (F).
R_{DC} : DC-link resistance (Ω).
α_{Batt} : Battery duty cycle.
α_{SC} : Super-capacitor duty cycle.
$V_{s\alpha,\beta}$: Stator α-β frame voltage (V).
$I_{s\alpha,\beta}$: Stator α-β frame current (A).
$\emptyset_{s\alpha,\beta}$: Stator α-β frame flux (Wb).
$E_{s\alpha,\beta}$: Stator α-β frame back EMFs (V).
L : Stator inductance (H).
R_s : Stator Resistance (Ω).
T_e : Electromagnetic torque (Nm).
T_L : Load torque (Nm).
f : Viscous damping coefficient (N m rad−1 s).
p: Number of pole pairs.
Ω: Synchronous mechanical speed (rad s−1).
ω: Synchronous electrical speed (rad s−1).
We_V_{DC}, We_V_{SC} : Performance weighting functions.
Wu_I_{Batt}, Wu_I_{SC} : Control weighting functions.
$K(\rho)$: Feedback controller.
y : Measured outputs.
u : Control inputs.
w : exogenous inputs.
z : controlled outputs.

I. INTRODUCTION

Since the end of the 20th century, rising oil prices and environmental issues led the automotive industry to develop new efficient technologies, which generate zero gas emissions. Among these technologies, electric vehicles (EV) are a sustainable and efficient solution [1]. Generally, batteries are used as the primary energy source, which have a high energy density and store most of the on-board electrical energy. The major disadvantage of these batteries is their slow dynamics, which makes it necessary to use super capacitors (SCs) as an auxiliary source [2]. This association can enhance the performance of the hybrid energy storage system (HESS), by having more power density and being able to provide high peak currents.

In this context, the combination of such sources having different dynamics remains a challenge for researchers and engineers [3]. An energy management strategy (EMS) should ensure efficient performance that provides the best solution from a technical and economic point of view. An effective EMS

allows the vehicle to meet instantaneous power demand, increases the lifespan of storage elements, reduces the operating costs; therefore, optimizes the system performance and enhances the vehicle autonomy.

Several control algorithms used in the EMS have been studied in the literature, which are classified into rule-based strategies (RBS), frequency-based strategies (FBS), and optimization-based strategies (OBS). The RBS can also be divided into deterministic strategies (DS) and artificial intelligence (AI) based strategies. The DS are designed manually and developed without prior knowledge of the driving cycle. In contrast, the FBS schemes are particularly suitable for EVs due to the consideration of the dynamics of different sources. The OBS can be further divided into local optimization strategies (LOS), i.e., real-time optimization strategies, global optimization strategies (GOS), and offline optimization strategies (OOS) [4]. Nevertheless, the characteristics of an EMS according to a different point can be summarized, as shown in Fig. 1. As observed in Fig. 1, RBSs split the power between the involved sources using a set of rules based on human expertise. In [5], a DS rule-based strategy has been proposed, where the battery reference power is determined by both the SC state of charge (SOC) and the vehicle speed. This strategy is divided into different modes in order to share the power demand as well as to limit the power variation rate which increase the lifetime of both sources. RBSs are flexible and easy to implement; however, they rarely achieve optimal control. Another way to optimize RBSs is to combine it with AI approaches.

Several AI-based methodologies have been implemented such as fuzzy logic supervisors [6], neural network (NN) algorithms [7] and genetic algorithm (GA) [8]. The difficulty of obtaining accurate models of the HESS as well as predicting their SOC make these methodologies an unpractical tool. Furthermore, in [9], authors have considered a fuzzy logic supervisor that depends on the vehicle power demand, where the main objective is to avoid stressing the batteries. Other fuzzy logic-based algorithms have also been developed for HESS [10]-[11].

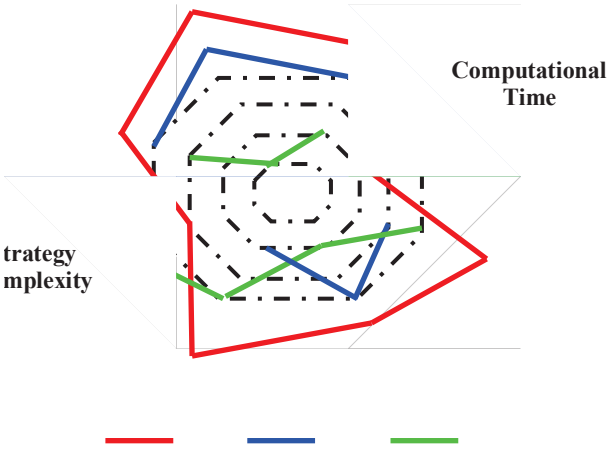

Fig1: EMS characteristics.

Those methods depend on the load current and the SOC of the SCs, and they does not take into account the frequency variation of the battery current. More recently, the multi-agent systems (MAS) were widely used for the HESS, especially in industrial applications. This type of approaches has been successfully implemented in real-time applications [12]. Additionally, FBSs are commonly used due to the slow response time of batteries, which cannot cover the fast power variations in EV applications. This strategy aims to separate the power consumption into high and low frequencies, where batteries must supply low frequencies of the power demand and the SCs respond to the high frequencies. For instance, Dusmez [13] employed filters to share the energy between three power sources. The first one is a low pass filter used to get the Fuel Cell (FC) reference current, while the second one is a high pass filter for splitting the remaining energy between the battery and the SC. Moreover, Zhang [14] proposed a discrete wavelet transform (DWT)-based method for the EMS to divide the power between FC, batteries, and SCs. The DWT method performed the spectral decomposition of the requested power, including the decomposition phase and the reconstruction phase. The interest in OBS research is increasing because of its ability to achieve optimal results. These results are calculated using a strategy that minimizes the sum of objective functions over time (global optimization) or by instantly minimizing an objective function (local optimization) [15].

In addition, various algorithms have been already studied such as the optimal control algorithm (OC), Pontryagin maximum principle (PMP) and dynamic programming (DP). DP strategies for the HESS have been widely investigated in the literature [16]. These algorithms guarantee a global optimality by finding an optimal control sequence to obtain the desirable value of SOC quantities, while minimizing the battery current over a given driving cycle. The OBS can significantly reduce HESS power consumption by avoiding transient loading and contributes to saving their SOC. Hence, the impact of the two issues has a significant impact on the computational time. This drawback makes it impractical in online applications, and some of these are very complex, making the design challenging in automotive devices.

Furthermore, a PMP has been studied in [17]; It is rformed by a Hamiltonian function, where a set of timization conditions are presented. In this approach, the mber of non-linear differential equations is determined by the e of the problem. Under certain assumptions, the PMP can so be used as an optimal overall strategy. Other EMS algorithms based on the model predictive control (MPC) were validated on dSPACE system, in order to solve the EMS issues for various configurations, e.g., FC/battery, FC/battery/SC and battery/SC [18]-[19]. Optimization-based strategies may outperform RBS in terms of efficiency and accuracy. However, their implement-ability is limited due to the heavy computational burden, as they require a large amount of data. Besides, these strategies may have a slow convergence speed and thus they may become locked into a local optimum, specifically for a longer interval horizon. The performance improvement of these algorithms is therefore limited. Across all reported research, the parametric variation was not clearly discussed in the EMS design, although there is a clear correlation between the parametric variation and optimum set

point in terms of power consumption. This means that an on-board power source cannot be optimized without considering the effect of the parametric variation.

Among the above-discussed methods, the parametric variation, computation time, robustness and stability should be the most challenging issues in real time implementation. Thus, a rising concern has been shown for the linear parametric variation (LPV) system as an effective solution to such problems. In the same vein, this paper proposes a novel EMS based on the LPV/H∞ approach, which ensures an optimum power flow between the involved power sources; in addition, to a smooth permutation between the different operating modes. The HESS under study consists of a battery pack, acting as the main source and two SC modules as an auxiliary source. The battery pack is connected to a common DC link through an interleaved buck-boost converter, while the SCs side is handled with a conventional buck-boost converter. The EMS is based on a polytopic formulation of a multi-input-multi-output (MIMO) system, where the inputs are the DC bus and the SC reference voltages, and the outputs are the reference current sources.

The main advantages of the proposed approach can be twofold. On the source side:

- A global asymptotic stability of the closed-loop system using the correct weighting functions is studied.
- Providing a quite regulation of the DC-Link and the SC voltage quantities without adding any extra controllers that permits to implement the algorithm under a shorter time.

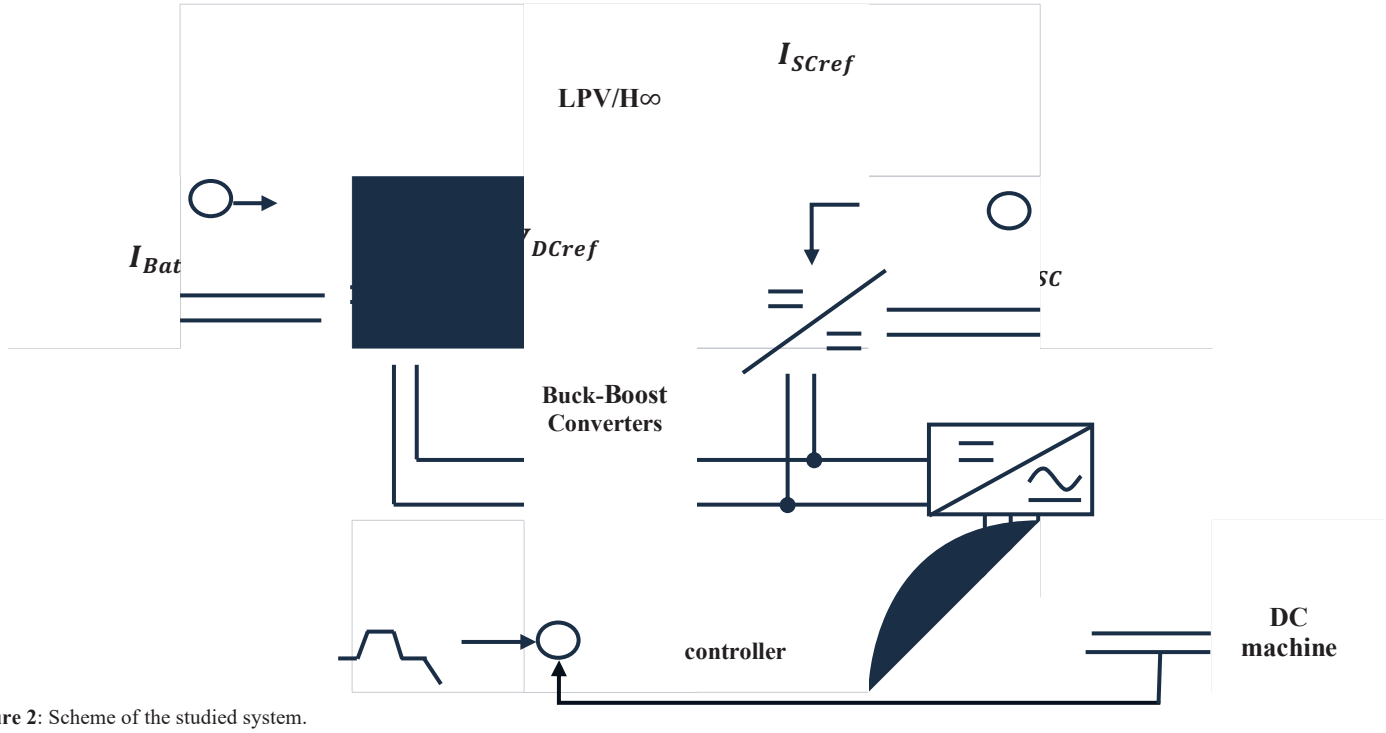

Figure 2: Scheme of the studied system.

- A power frequency separation is achieved, where the high-frequency variation is handled by the SCs, and the battery must supply the steady-state current (mean value).
- A flexible intelligent EMS based algorithm is developed which provides a compromise between real-time implementation and its ability to be compiled in all EVs by only adjusting the controller gains.

On the traction part, to extend this work to an automotive application, a set of permanent magnet synchronous motor (PMSM) coupled with a DC machine is integrated into the system, that emulates properly the vehicle's mission cycle. The motor control technique is performed via a back-stepping direct torque control (BTDTC), using a two-level voltage source (VS) inverter. According to a quite choice of recursive Lyapunov functions, the VS inverter is tuned via a space vector modulation technique (SVM) in order to accomplish speed, torque, and stator flux regulation. The main contributions can be summarized as follows:

- A new solution to the problem of EMSs for HESS with potentially any number of energy sources is proposed, while managing the parametric variation of this system.
- The originality of the frequency separation technique is based on the weighting functions associated to the LPV controller. It can go beyond conventional methods that use low-pass and high-pass filters, adaptive filters and the DWT method. The proposed technique can solve any energy coordination problems thanks to its powerful combination between optimization and filtering while dealing with parametric variation, it is flexible, by adding the number of parameters in proportion to the number of sources used.
- The proposed supervisor does not require any prediction or estimation of the load current which is a strong point compared to other EMSs. Therefore it can be applied to other EVs with any speed profile.
- A global system control, in both sources and traction sides, inspired from the control theory (LPV/Back- stepping control) to tune the static converters under realistic conditions.

This kind of implementation can be a real challenge to replace conventional control algorithms applied to heavy industrial vehicles.

The rest of the paper is organized as follows. Section II presents the explicit models of the different sub-systems. Section III describes the proposed control algorithms. Section IV presents the simulation and the experimental results, while Section V concludes the work.

II. System modeling

A. Input stage:

The first stage encompasses the involved power sources, as depicted in Fig. 2. For the SC source, various models exist in literature. Among them, a simple model represented respectively by Eqs. (1) and (2) that reproduce the electric behavior of such device with acceptable accuracy. The three parameters, *ESR*, V_0 and C_{SC} represent the Equivalent Series Resistance, the open circuit voltage and the SC capacitance. These parameters, given in appendix, were identified by the recursive least square method (RLS), using a successive pulsed discharge current. For the battery pack, a simple model is given in (3), adopted for Lead Acid battery modeling. It introduces only the ohmic effect, via the resistance R_{Batt} in order to distinguish the output voltage V_1 over the open circuit voltage E_0.

$$V_{SC} = V_0 - ESR.I_{SC} \quad (1)$$

$$\frac{dV_0}{dt} = \frac{I_{SC}}{C_{SC}} \quad (2)$$

$$E_0 = V_1 - R_{Batt}.i_{Bat} \quad (3)$$

B. Conversion stage:

In order to implement the proposed control in a continuous model, the average state space approach is adopted to represent the dynamic behavior of the converters. These models provide the current/voltage evolution of each storage element (inductance/capacitor), taking as a parameter for the duty cycle.

$$\frac{dI_{SC}}{dt} = \frac{1}{L_{SC}}[V_{SC} - ESR.I_{SC} - V_{DC}(1-\alpha_{SC})] \quad (4)$$

$$\frac{dI_{Batt}}{dt} = \frac{1}{L_{Batt}}[V_{Batt} - R_{Batt}.I_{Batt} - V_{DC}(1-\alpha_{Batt})] \quad (5)$$

C. Output stage:

The provided power quantities of both sources are collected on the common DC link, where Eq (6) depicts the dynamic power balance.

$$\frac{dV_{DC}}{dt} = \frac{1}{C_{DC}}\left[I_{Batt}.\alpha_{Batt} + I_{SC}.\alpha_{SC} - I_{Load} - \frac{V_{DC}}{R_{DC}}\right] \quad (6)$$

In which R_{DC} represents the equivalent load resistance sensed at the DC-link.

D. Motor stage:

Assuming a functioning under no magnetic saturation and no core losses, the electrical and mechanical dynamic models of the synchronous machine in the stationary reference (α-β) frame are given as

$$V_{s\alpha} = R_s.i_{s\alpha} + L\frac{di_{s\alpha}}{dt} + E_\alpha \quad (7)$$

$$V_{s\beta} = R_s.i_{s\beta} + L\frac{di_{s\beta}}{dt} + E_\beta \quad (8)$$

$$p(T_e - T_L) = J\frac{d\omega}{dt} + f.\omega \quad (9)$$

where the back EMFs and are deduced as:

$$E_\alpha = w.\emptyset_f(-sin\theta) \quad (10)$$

$$E_\beta = w.\emptyset_f(\cos\theta) \quad (11)$$

The electromagnetic torque expression can be obtained through the multiplication of the global stator flux and currents, as given in (12). In case of salient machine, this equation contains the synchronous component as well as the reluctant component:

$$T_e = \frac{3}{2}p\left[i_\beta.\emptyset_{s\alpha} - i_\alpha.\emptyset_{s\beta}\right] \quad (12)$$

The gradient of the stator flux linkage components is easily obtained via the Kirchhoff's law:

$$\dot{\emptyset}_{s\alpha} = V_{s\alpha} - R_s.i_{s\alpha} \quad (13)$$

$$\dot{\emptyset}_{s\beta} = V_{s\beta} - R_s.i_{s\beta} \quad (14)$$

Finally, the amplitude of the stator flux is obtained:

$$\emptyset = \sqrt{{\emptyset_{s\alpha}}^2 + {\emptyset_{s\beta}}^2} \quad (15)$$

III. Control design

A. LPV based supervising strategy

In order to properly manage the system in various operating scenarios (e.g., acceleration/deceleration, and steady state), the proposed robust control is used. The philosophy is to design a robust gain-scheduled controller K(ρ), ensuring a global asymptotic stability of an affine linear system, regardless the variation of the bounded parameters (ρ). Assuming a real time calculation of these parameters, the feedback gain K(ρ) is then evaluated in real time as a function of the 2^n system vertexes. The introduced LPV controller should adequately share the load demand between the involved sources in every operation mode, while respecting their dynamics. The control objectives are then summarized as follows:

- Ensuring a total power flow to the load, with the regulation of the DC bus voltage around a set value (60 V), regardless the motor speed variation.
- Preserving the maximum power availability of the SC module during repetitive peak current, by regulating the SCs voltage around (2/3). V_{SC_mqx}.
- Applying a power frequency splitting to the involved sources. In this context, each source should provide energy according to its dynamics. Thus, the battery pack is protected from rapid and harmful variations. The frequency splitting is achieved by a careful choice of the weighting functions associated with the design of the LPV/H∞ control.

The Linear fractional transformation (LFT) of the control diagram is shown in Fig.3. It includes the augmented power plant P(ρ), and the feedback controller K(ρ). The exogenous inputs (W) are included in the DC-link V_{DC_ref} and the SC voltage set points V_{SC_ref}. In addition the load current I_{Load} is considered as a disturbance input. The output (Z) gathers the tracking errors of the DC-link and the SC voltage amount, while

This article has been accepted for publication in a future issue of this journal, but has not been fully edited. Content may change prior to final publication. Citation information: DOI 10.1109/TEC.2020.3017811, IEEE Transactions on Energy Conversion

the control inputs are the battery and SC reference currents I_{Batt_ref}, I_{SC_ref}. The design of the controller gain K(ρ) is performed along the famous loop shaping H∞ strategy, where the performance and control are set across the weighting functions, respectively, (We_V_{DC}, We_V_{SC}) and (Wu_I_{Batt}, Wu_I_{SC}). These quantities are generally chosen as low and high pass filters, according to each control purpose. To ensure a perfect regulation of V_{DC} and V_{SC}, the performance weighting functions are chosen as low pass filters:

$$\frac{1}{We\_V_{DC}} = \frac{s+0.5}{0.5s+5000} \quad (16)$$

$$\frac{1}{We\_V_{SC}} = \frac{s+0.005}{0.5s+5} \quad (17)$$

where the dynamic performance can be tuned via a proper choice of the pass band frequency, respectively, 50 rad/s and 100 rad/s. In order to perform a power frequency separation, the control weighting functions are set accordingly. The battery is asked to cover the load demand in steady states, and consequently, the related function is a first order low pass filter. Due to the skills of the SC in covering the dynamic demand, a high pass first order filter is used:

$$\frac{1}{Wu\_I_{Batt}} = \frac{s^2+25s+1}{5s^3+5s^2+s+1} \quad (18)$$

$$\frac{1}{Wu\_I_{SC}} = \frac{s^2+30s+1}{10s^3+s^2+10s+1} \quad (19)$$

Figure 3: LFT representation of the LPV plant.

The sate space modeling of the system is represented as

$$\dot{x} = Ax + B_1 w + B_2(\rho)\, u \quad (20)$$

$$y = Cx + D\, u \quad (21)$$

where:

$x = [V_{DC}\ \ V_{SC}]^T$

$u = [I_{Batt}\ \ I_{SC}]^T$

$w = I_{Load}$

$\rho = [\alpha_{Batt}\ \ \alpha_{SC}]^T$

The transition matrix A, the associated control and disturbance matrices B_1, B_2, C and D are deduced as:

$$A = \begin{bmatrix} \frac{-1}{R_{DC}C_{DC}} & 0 \\ 0 & 0 \end{bmatrix}, B_1 = \begin{bmatrix} \frac{-1}{C_{DC}} \\ 0 \end{bmatrix}, D = \begin{bmatrix} \frac{\alpha_{Batt}}{C_{DC}} & \frac{\alpha_{SC}}{C_{DC}} \\ 0 & \frac{-1}{C_{SC}} \end{bmatrix}$$

$$C = \begin{bmatrix} 1 & 0 \\ 0 & 1 \end{bmatrix}$$

$$B_2 = \begin{bmatrix} 0 & 0 \\ 0 & -R_{SC} \end{bmatrix}$$

As can be noticed, the chosen variant parameters are the two duty cycles related to each DC-DC converter, computed in real time and bounded as follows:

$$0.05 < \alpha_{Batt} < 0.95 \quad (22)$$

$$0.05 < \alpha_{SC} < 0.95 \quad (23)$$

Furthermore, in Eq. (20), the control input matrix B_2 is a parameter dependent, which is not consistent with the solution of the H∞ design problem for polytopic systems. In order to solve this problem, an augmented state space model is made using a first order low pass filter (see Fig. 4), with a enough large band pass:

$$\begin{pmatrix} \dot{x}_f \\ u_f \end{pmatrix} = \begin{pmatrix} A_f & B_f \\ C_f & 0 \end{pmatrix} \begin{pmatrix} x_c \\ u_c \end{pmatrix} \quad (24)$$

u_c

Figure 4: Augmented Linear design.

According to Eqs. (20) and (24), the system is now represented by an LPV formula given in Eq. (25), focusing on the design of a polytopic controller considering the convex set of bounded parameters ($\alpha_{Batt}, \alpha_{SC}$).

$$\dot{x} = A(\rho_1, \rho_2)x + B_1 w + B_2\, u_c \quad (25)$$

$$y = Cx \quad (26)$$

This task starts from an affine representation of the different matrices, as the function of 2^ρ vertexes.

$$A(\rho) = A_0(p) + \sum_1^4 \alpha_i(\rho) A_i \quad (27)$$

$$B(\rho) = B_0(p) + \sum_1^4 \alpha_i(\rho) B_i \quad (28)$$

$$C(\rho) = C_0(p) + \sum_1^4 \alpha_i(\rho) C_i \quad (29)$$

$$D(\rho) = D_0(p) + \sum_1^4 \alpha_i(\rho) D_i \quad (30)$$

with $\sum_1^4 = 1$ and $\alpha_i(\rho) = \frac{\Pi_{j=1}^2 |\rho_j - c(wi)_j|}{\Pi_{j=1}^2 |\bar{\rho}_j - \underline{\rho}_j|} > 0$.

The dynamical LPV system can be reformulated as

$$\begin{bmatrix} \dot{x} \\ z \\ y \end{bmatrix} = \begin{bmatrix} A & B_1 & B_2(\rho) \\ C_1 & D_{11} & D_{12} \\ D_2 & D_{21} & D_{22} \end{bmatrix} \begin{bmatrix} x \\ y \\ z \end{bmatrix} \quad (31)$$

where (y) denotes the measured output, (w) the exogenous inputs, (z) indicates the controlled outputs, and (u) represents the control inputs. The related feedback controller $K(\rho)$ is written as a linear relationship of the four vertexes K_i, computed across the loop shaping $H\infty$:

$$K(\rho) = \sum_1^4 \alpha_i(\rho) K_i \quad (32)$$

$$K(\rho) = \sum_1^4 \alpha_i \begin{bmatrix} A_K(\pi_i) & B_K(\pi_i) \\ C_K(\pi_i) & D_K(\pi_i) \end{bmatrix} \quad (33)$$

This structure is designed to achieve Lyapunov's quadratic stability, and satisfies the desired performances thanks to the convex optimization. The LPV controller can be expressed in state space as:

$$K(\rho): \begin{pmatrix} \dot{x}_f \\ u_c \end{pmatrix} = \begin{pmatrix} A(\rho) & B(\rho) \\ C(\rho) & D(\rho) \end{pmatrix} \begin{pmatrix} x_c \\ y \end{pmatrix} \quad (34)$$

where x_c is the state, y is the input, and u_c is the output of the controller.

To achieve the mentioned objectives, the L_2 norm given in (35) is taking into consideration, by reducing the impact of the exogenous input (ω) on the controlled output (Z):

This article has been accepted for publication in a future issue of this journal, but has not been fully edited. Content may change prior to final publication. Citation information: DOI 10.1109/TEC.2020.3017811, IEEE Transactions on Energy Conversion

$$\left\|F_l\left(G(\rho)\right), K(\rho)\right\|_\infty = sup\frac{\|Z\|_2}{\|u\|_2} \leq \gamma. \quad (35)$$

According to [20], the output feedback controller presented in (34) must solve the set of linear matrix inequalities (LMIs) (36), and (37) in the meantime minimizing γ.

$$\begin{bmatrix} XA_j + B_{2j}C_2 + * & * & * & * \\ \hat{A}_{kj}^T + A_j & A_jY + B_{2j}C_{kj} + * & * & * \\ \left(XB_{1j} + \hat{B}_{kj}D_{21}\right)^T & B_{1j}^T & -\gamma I & * \\ C_{1j} & C_{1j}Y + D_{12}\hat{C}_{kj} & D_{11} & -\gamma I \end{bmatrix} < 0 \quad (36)$$

$$\begin{bmatrix} X & I \\ I & Y \end{bmatrix} > 0. \quad (37)$$

where

$$A_{kj} = N^{-1}\left(A_{kj} - XA_jY - B_{kj}C_{2j}Y - XB_{2j}C_{kj}\right)M^T \quad (38)$$

$$B_{kj} = N^{-1}\widehat{B_{kj}} \quad (39)$$

$$C_{kj} = \widehat{C_{kj}}M^{-T} \quad (40)$$

in which N and M are two matrices that satisfy

$$I - XY = NM^T \quad (41)$$

The performance and the stability of the robust controller are ensured, if the disturbance rejection, or more precisely the effect of the exogenous inputs (W) on the (Z) filtered outputs is attenuated below the ratio 1.

B. Steps into the solution

The LPV/H∞ control synthesis is a disturbance attenuation problem. It consists in finding a stabilizing controller that minimizes the impact of the exogenous inputs W (V_{DC_ref} and V_{SC_ref}) on the controlled output Z which gathers the tracking errors of the DC-link and the SC voltage amount. In the case of the H∞ control, this impact is measured thanks to the induced L2 norm. To do this, several steps must be respected to solve the problem as resumed in the flowchart (see Fig. 4).

IV. SIMULATION AND EXPERIMENTAL RESULTS

To assess the feasibility of the proposed method, a small-scale system was designed, using two lead-acid batteries (100 Ah/12 V) and two Maxwell SC modules (52 F/16V), as shown in Fig. 5. The load is emulated by a permanent magnet synchronous machine of 400 W rated power, fed through a Semikron voltage source didactic inverter. In an analog way, The DC-DC power converters are made using the 4-kW didactic Semikron converter, which associates three SKM50123 IGBT modules, connected to a common dc bus. All these devices have the advantage to obtain the accessibility to the related SKHI22 Driver in order to separate the control of each module. The control algorithms are implemented using two TMS32F240 cards from Texas Instrument, in which each card performs the control of one side. The control gains are based on the duty cycles α_i and the vertexes K_i which cannot be computed online via LMIs. For this purpose, an offline calculation , taking into account a matrix of 5 by 5, i.e. 25 gains that sweep all the duty cycle values ($\alpha_{Batt}, \alpha_{SC}$), the control algorithm has been implemented with a sampling time equal to 150 µs. It is noteworthy mentioning that the PMSM is loaded with a DC machine for emulating the vehicle behavior. The speed sensor is an incremental encoder with 1024 pulses/revolution, and the LEM sensors used for current and voltage measurements are respectively LA-55NP and LV-25P.

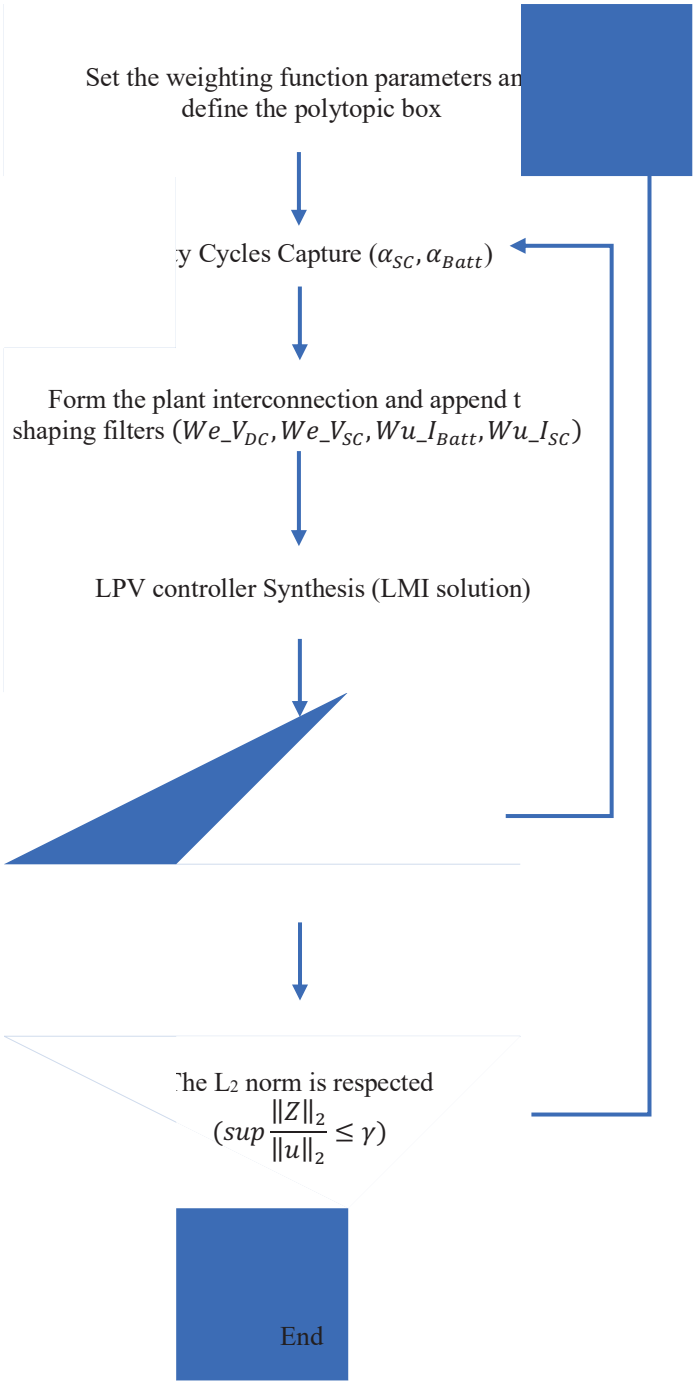

Figure 4: Control design flowchart.

This article has been accepted for publication in a future issue of this journal, but has not been fully edited. Content may change prior to final publication. Citation information: DOI 10.1109/TEC.2020.3017811, IEEE Transactions on Energy Conversion

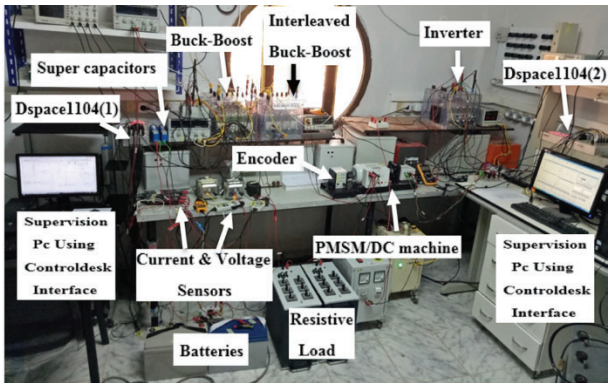

Figure 5: Experimental test bench.

In order to allow an easier reading of the obtained experimental findings, a variable speed profile is applied, containing repetitive accelerations during the time window [0-2s], [7.5-9s], [12-13s]; then, constant speeds between [2-5s], [5.5-7.5s], [9 - 11s], and finally several decelerations between [5-5.5s], [11-12 s] (see Fig. 6). The assessment of the proposed control techniques is achieved by comparing the simulation and experimental results.

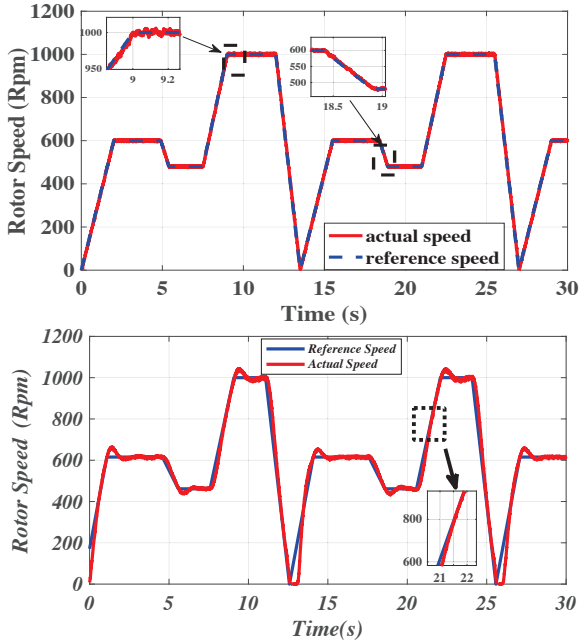

Figure 6. Speed profile: (a) simulation results and (b) experimental results.

In the course of the chosen speed profile, the following remarks are extracted:

- During the first interval, where the EV accelerates from 0 rpm to 600 Rpm, the motor speed tracks adequately the reference speed during the transient state (see Fig. 6), in both simulation and experiment results. Once the reference speed achieves the constant mode, a small overshoot over the time span is remarked. This result can be explained by the choice of the back-stepping control gains, respectively k_ω, k_{Te} and $k_\emptyset$. It is worth investigating, that after a set of tests, the adopted gains given in appendix provide suitable system performances.
- During the remaining time windows, where constant and fast deceleration operating modes were planned, the same remarks are made, regardless the load torque evolution, which proves consequently the effectiveness of the proposed control technique.

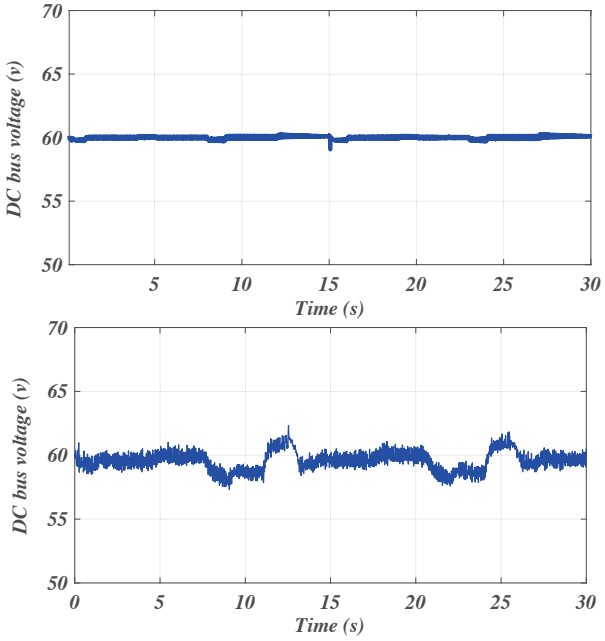

Figure 7. DC bus voltage: (a) simulation results and (b) experimental results.

To evaluate the proposed LPV power management routine skills, the supervisor performances will be concluded to regulate both DC-link and SC voltages and perform the power splitting. By analyzing the shape of the speed profile, that consists of many rising and falling edges. This severe profile is typically a vehicle's current demand in a real urban trajectory. At a starting point, the investigation will be focused on the transient response of the system. The EMS enhancement of the HESS under the proposed LPV supervisor can be assessed, using the plot of both the DC-link and SC voltages over the time span, as depicted in Fig. 7 and 8, respectively. As it can be noticed in Fig. 7 and 8, the LPV supervisor success, via an adequate weighting functions to maintain both the DC-link and the SC voltage amounts around their set values, 60 V and 26 V, respectively. To respect the dynamic behavior of each source, it is worth noting that the DC-link voltage regulation is guaranteed using a slower cut-off frequency filter compared to the SC one.

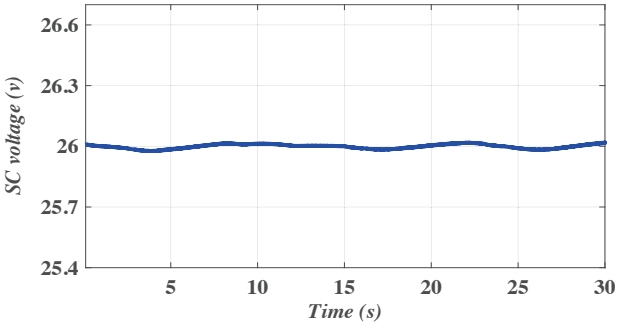

This article has been accepted for publication in a future issue of this journal, but has not been fully edited. Content may change prior to final publication. Citation information: DOI 10.1109/TEC.2020.3017811, IEEE Transactions on Energy Conversion

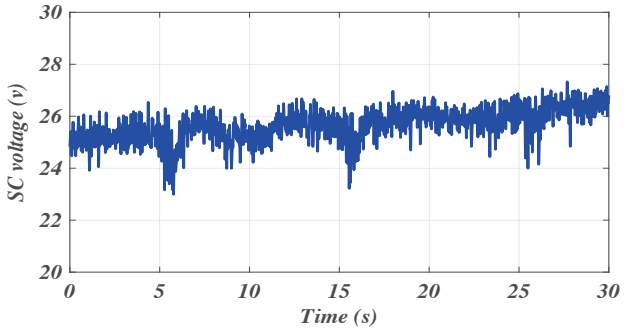

Figure 8. SC voltage: (a) simulation results and (b) experimental results.

When the motor accelerates at (t = 0 s and 7 s), the SC reacts immediately and supplies the transient energy demand in a short time as displayed in the current shape of Fig. 8, whereas the batteries slowly provide a current amount as shown in Fig. 9, to adjust the SC voltage around its reference value 26 V.

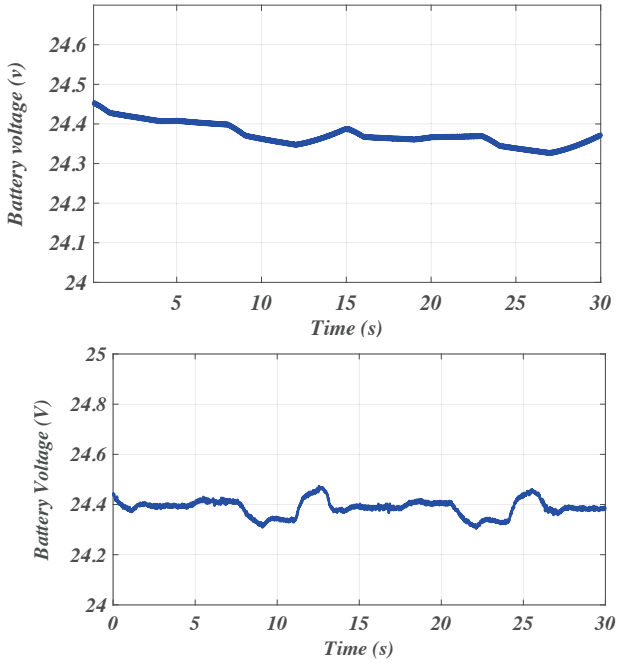

Figure 9. Battery voltage, (a) simulation results, (b) experimental results.

In contrast to that scenario, where a speed decrease is noticed, respectively, at t = 22s, and t = 25s, the SC voltage recharges through a negative current, which is recovered by the braking process (see Fig. 10). The SC would stay recharging with the negative power until the motor accelerates. If the SC voltage is larger than V_{SC_ref}, the LPV supervisor switches to the first mode, that permits the battery to provide the DC component of the load current. Whereas, the SC modules provide positive transient currents until they will be discharged under the set voltage.

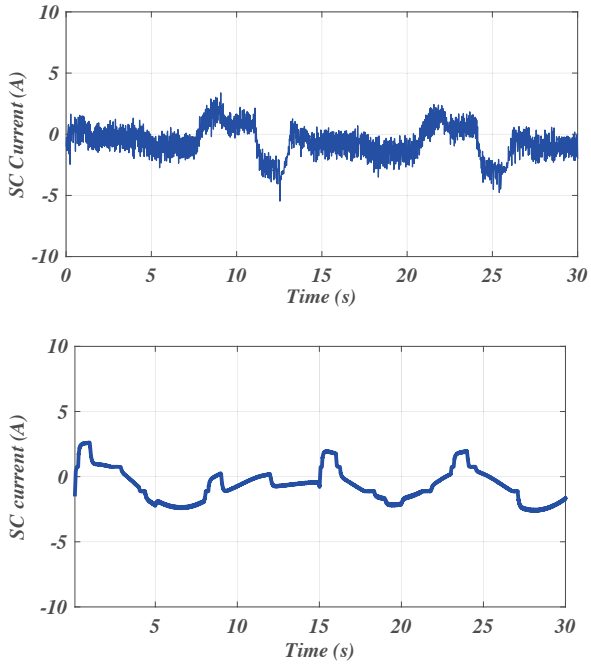

Figure 10. SC current, (a) simulation results, (b) experimental results.

During the instants [0s,7s and 20s], the battery provides the required motor current and regulates the SC voltage at the meantime (Fig. 11), meaning so operation in first mode. These three modes allow the regulation of the SC voltage around an optimal point (V_{SC_ref} = 26V).

During the instants [5s,12s and 25s], where the motor asks for low current amount, the battery current drops to a small value (2.5 A), indicating the second mode operation. In this case, there is no charge of the SC because this latter is recharged by the deceleration current.

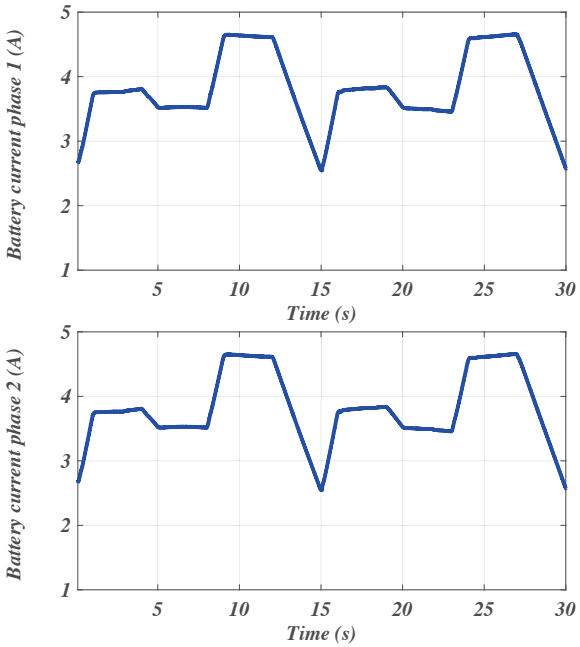

This article has been accepted for publication in a future issue of this journal, but has not been fully edited. Content may change prior to final publication. Citation information: DOI 10.1109/TEC.2020.3017811, IEEE Transactions on Energy Conversion

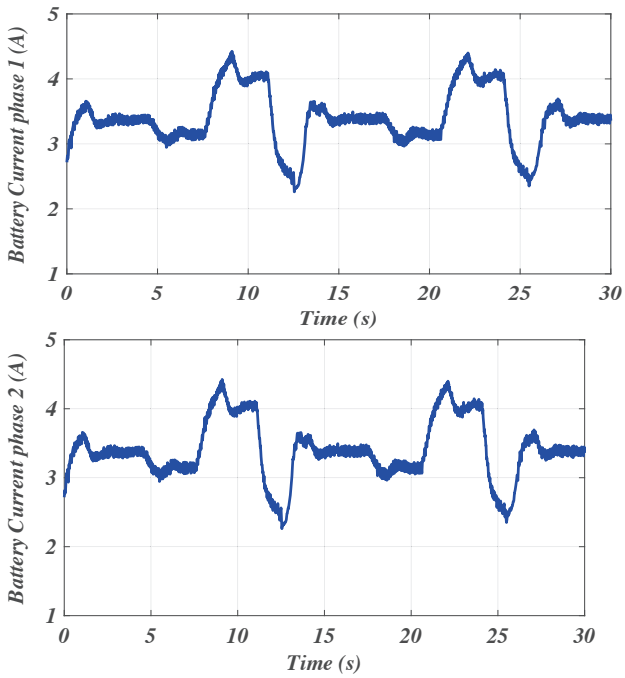

Figure 11. Battery current, (a). (b) simulation results, (c). (d) experimental results.

During the last part of the profile [7.5s-10s], the battery current stays lightly as the first one, while the SC provides positive current. The system here switches to the third mode. In this case, the requested SC current remains positive while its voltage is higher than the nominal value. The main source current I_{Batt} is divided into two phases in order to protect the converter in case of high motor demand. The two currents (see Fig 11) are perfectly similar and they are inverse to the battery voltage during the speed profile. It can be seen that the battery is working in a safe voltage region (24 v) which prolongs its lifetime.

V. Comparative study

EMSs are mainly based on splitting the power and at the same time respecting the dynamical properties of each source in the HESS. However, with the development of both control theory and artificial intelligence, scientists must adapt to this evolution by involving these two aspects in EV. Therefore, a precise understanding of source operating modes facilitates the choice of an appropriate algorithm and avoids the complexity of the system. In this subsection, a comparative study will be carried out, including some criteria mentioned in our previous work. The comparison focuses on supervisor robustness, tracking speed, energy sharing, complexity of implementation and required sensors. To perform this comparative study, a fuzzy logic power supervisor used in our previous works is considered [10].

Subsequently, it has been demonstrated that the speed profile produces I-V stresses at the sources side. However, most of the recent works did not test a concrete comparison between different supervisors. For the present comparison, the experimental results were obtained from the same HESS.

In order to test the tracking speed of these twos algorithms, two main criterions are calculated:

- The number of times 'hit count', which correspond to the number of times the DC-link voltage was calculated to reach its reference value.
- The integral absolute error IAE, calculated as the absolute surface area to track the DC-link reference value.

$$IAE = \int_{O}^{t} |e(t)|dt \qquad (42)$$

where e(t) denotes the tracking error.

Therefore, the two methods listed in Table 1 were tested using a similar speed profile. To evaluate each method skills in the steady state, the following performances indexes are defined:

- The DC-link voltage ripple (rip), testing the softness around the reference voltage. It is calculated as the ratio of the difference between the highest and the lowest voltage peaks, reported to the average DC-link voltage.

$$rip(\%) = (V_{DCmax} - V_{DCmin})/V_{DCref} \qquad (43)$$

- The tracking accuracy, evaluated as the ratio of the DC-link voltage calculated by each algorithm in steady state, and the reference voltage value.

$$\eta(\%) = V_{DC}/V_{DCref} \qquad (44)$$

To shed light on the obtained results, Table 1 identifies some performances indicators computed for the mentioned LPV and Fuzzy logic supervisors.

Table1: Comparison of EMS based algorithms.

Methods	LPV	Fuzzy
IAE	0.079	1.726
Hit-count	15	35
Tracking accuracy	98.37%	63.07%
Voltage ripple	0.02%	2.86%
$\boldsymbol{max_{acc}}$	99.96%	70.04%
$\boldsymbol{min_{acc}}$	96.78%	56.11%

The success of the follow-up was defined as 98.37% which is higher than our past work. Hence, the accuracy of monitoring should also be considered in assessing the supervisor's performance. The average accuracy is obtained during 10 tests of the tracking process for each method. Thus, it is the iteration ratio that corresponds to $V_{DC} = V_{DC\_ref}$ divided by the number of the performed tests. Similarly, the maximum accuracy (max_{acc}) and the minimum accuracy (min_{acc}) refer to the maximum and minimum values of the 10 test results respectively. In addition to the tracking accuracy, the tracking speed is also essential for the comparative study to test the softness of the various variables in steady state.

The advantage of the LPV supervisor is that it allows through the off-line calculation of the gains, the right choice of performance weighting functions and the use of the loop-shaping approach, to reduce the response time, on the other hand the fuzzy logic supervisor and through its blocks of inferences, fuzzification and defuzzification will take an

additional time of calculation.

Table 2: Performance indicators of EMS algorithms.

Methods	LPV	Fuzzy
Robustness	Yes	No
Tracking speed	Fast	Medium
Hit count	Low	High
Algorithm complexity/ sampling time	Yes Ts=150μs	No Ts=100μs
Power sharing	Smooth	Moderated
Sensors required	Voltage and current	Voltage and current
Dependence on model	Yes	No

As has been pointed out in Tables 1 and 2, the low values of the IAE performance indices and the hit count clearly show a fast dynamic response of the proposed LPV algorithm, where the algorithm is computed in only 15 iterations to reach the reference value. The LPV results show that the DC-link voltage follows perfectly its reference value in a few milliseconds, and with an acceptable overshoot compared to the fuzzy logic.

For instance, in order to choose the appropriate sampling time, the supervisor's experimental validation must consider the stabilization time of the power electronic circuit. If the sampling time is faster than the system stabilization time, the value of both voltage and current sampled by the algorithm does not indicate the steady state. As a result, they cannot be used to evaluate the effects generated by the control algorithm. However, the stabilization time of a low power converter is shorter; therefore, the tracking time will also be the same. In other words, assessing the tracking speed of the two supervisors by comparing them without taking other factors into account produces erroneous results. Thus, we proposed using the number of iterations required only to compare tracking speeds.

VI. Conclusion

In this paper, a new robust control for small-scale EVs has been detailed. This work involves the power management of a HESS for EV application. The EMS was based on the LPV approach, where the power coordination has been carried out and validated according to the dynamics of each involved source. On the traction part, a DTCBS based technique was adopted to control the PMSM. A speed profile was selected containing several acceleration and deceleration states to evaluate the control algorithms. The obtained experimental results prove the effectiveness of these control techniques, where a perfect power sharing between the used sources was ensured. The proposed algorithms are suitable for high power industrial applications with a simple adaptation of the controller's gains. In order to test the effectiveness of the proposed algorithms in a comparative way, a fuzzy logic- based technique was considered. The quantification of the various performance indexes demonstrates clearly a notable superiority of the LPV based power supervisor.

Appendix

Battery characteristics: (features provided by the manufacturer):

- Capacity=100 Ah.
- Maximum voltage: V=13.5 V.
- Minimum voltage=8.5 V.
- Internal resistance (Rbatt): 5mΩ.

Super capacitor characteristics

- Rated capacitance: 58 farad.
- Rated voltage: 16 V.
- Maximum voltage: V=17 V.
- Minimum voltage: V=11 V.
- Internal resistance (Rsc): 22mΩ.

PMSM characteristics

- Stator resistance 2Ω.
- D-axis inductance 43 mh.
- Rated power: 250 watts.
- Viscous damping coefficient 0.000054(Nm rad-1s)
- The number of pole pairs: 2.
- motor inertia 0.0008 (Kg m2)

Passive elements:

- C_{DC} =2200µF
- L_{SC} = 3mH, 20A.
- L_{Batt} = 10mH, 10A.

Backstepping gains:

- k_{ω}= 0.02.
- k_{Te}=40.
- k_{ϕ}=10.

References

[1] F. Akar, Y. Tavlasoglu, and B. Vural, "An Energy Management Strategy for a Concept Battery/Ultracapacitor Electric Vehicle With Improved Battery Life," *IEEE Trans. Transp. Electrification*, vol. 3, no. 1, pp. 191–200, Mar. 2017, doi: 10.1109/TTE.2016.2638640.

[2] M. Sellali, A. Betka, and A. Djerdir, "Power management improvement of hybrid energy storage system based on H ∞ control," *Math. Comput. Simul.*, vol. 167, pp. 478–494, Jan. 2020, doi: 10.1016/j.matcom.2019.05.003.

[3] M. W. Beraki, J. P. F. Trovao, M. S. Perdigao, and M. R. Dubois, "Variable Inductor Based Bidirectional DC–DC Converter for Electric Vehicles," *IEEE Trans. Veh. Technol.*, vol. 66, no. 10, pp. 8764–8772, Oct. 2017, doi: 10.1109/TVT.2017.2710262.

[4] H. Li, A. Ravey, A. N'Diaye, and A. Djerdir, "A novel equivalent consumption minimization strategy for hybrid electric vehicle powered by fuel cell, battery and supercapacitor," *J. Power Sources*, vol. 395, pp. 262–270, Aug. 2018, doi: 10.1016/j.jpowsour.2018.05.078.

[5] M. Zandi, A. Payman, J.-P. Martin, S. Pierfederici, B. Davat, and F. Meibody-Tabar, "Energy Management of a Fuel Cell/Supercapacitor/Battery Power Source for Electric Vehicular Applications," *IEEE Trans. Veh. Technol.*, vol. 60, no. 2, pp. 433–443, Feb. 2011, doi: 10.1109/TVT.2010.2091433.

[6] J. P. F. Trovao, M.-A. Roux, E. Menard, and M. R. Dubois, "Energy- and Power-Split Management of Dual Energy Storage System for a Three-Wheel Electric Vehicle," *IEEE Trans. Veh. Technol.*, vol. 66, no. 7, pp. 5540–5550, Jul. 2017, doi: 10.1109/TVT.2016.2636282.

[7] J. P. F. Trovao, V. D. N. Santos, C. H. Antunes, P. G. Pereirinha, and H. M. Jorge, "A Real-Time Energy Management Architecture for Multisource Electric Vehicles," *IEEE Trans. Ind. Electron.*, vol. 62, no. 5, pp. 3223–3233, May 2015, doi: 10.1109/TIE.2014.2376883.

[8] J. Shen and A. Khaligh, "A Supervisory Energy Management Control Strategy in a Battery/Ultracapacitor Hybrid Energy Storage System," *IEEE Trans. Transp. Electrification*, vol. 1, no. 3, pp. 223–231, Oct. 2015, doi: 10.1109/TTE.2015.2464690.

[9] Wenhao Zhou, M. Li, He Yin, and C. Ma, "An adaptive fuzzy logic based energy management strategy for electric vehicles," in *2014 IEEE 23rd International Symposium on Industrial Electronics (ISIE)*, Istanbul, Turkey, Jun. 2014, pp. 1778–1783, doi: 10.1109/ISIE.2014.6864884.

[10] M. Sellali, A. Betka, S. Drid, A. Djerdir, L. Allaoui, and M. Tiar, "Novel control implementation for electric vehicles based on fuzzy -back stepping approach," *Energy*, vol. 178, pp. 644–655, Jul. 2019, doi: 10.1016/j.energy.2019.04.146.

[11] M. Sellali, S. Abdeddaim, A. Betka, A. Djerdir, S. Drid, and M. Tiar, "Fuzzy-Super twisting control implementation of battery/super capacitor for electric vehicles," *ISA Trans.*, vol. 95, pp. 243–253, Dec. 2019, doi: 10.1016/j.isatra.2019.04.029.
[12] E. Xydas, C. Marmaras, and L. M. Cipcigan, "A multi-agent based scheduling algorithm for adaptive electric vehicles charging," *Appl. Energy*, vol. 177, pp. 354–365, Sep. 2016, doi: 10.1016/j.apenergy.2016.05.034.
[13] S. Dusmez and A. Khaligh, "A Supervisory Power-Splitting Approach for a New Ultracapacitor–Battery Vehicle Deploying Two Propulsion Machines," *IEEE Trans. Ind. Inform.*, vol. 10, no. 3, pp. 1960–1971, Aug. 2014, doi: 10.1109/TII.2014.2299237.
[14] X. Zhang, C. C. Mi, A. Masrur, and D. Daniszewski, "Wavelet-transform-based power management of hybrid vehicles with multiple on-board energy sources including fuel cell, battery and ultracapacitor," *J. Power Sources*, vol. 185, no. 2, pp. 1533–1543, Dec. 2008, doi: 10.1016/j.jpowsour.2008.08.046.
[15] N. Denis, M. R. Dubois, J. P. F. Trovao, and A. Desrochers, "Power Split Strategy Optimization of a Plug-in Parallel Hybrid Electric Vehicle," *IEEE Trans. Veh. Technol.*, vol. 67, no. 1, pp. 315–326, Jan. 2018, doi: 10.1109/TVT.2017.2756049.
[16] Zheng Chen, C. C. Mi, Jun Xu, Xianzhi Gong, and Chenwen You, "Energy Management for a Power-Split Plug-in Hybrid Electric Vehicle Based on Dynamic Programming and Neural Networks," *IEEE Trans. Veh. Technol.*, vol. 63, no. 4, pp. 1567–1580, May 2014, doi: 10.1109/TVT.2013.2287102.
[17] B.-H. Nguyen, R. German, J. P. F. Trovao, and A. Bouscayrol, "Real-Time Energy Management of Battery/Supercapacitor Electric Vehicles Based on an Adaptation of Pontryagin's Minimum Principle," *IEEE Trans. Veh. Technol.*, vol. 68, no. 1, pp. 203–212, Jan. 2019, doi: 10.1109/TVT.2018.2881057.
[18] O. Gomozov, J. P. F. Trovao, X. Kestelyn, and M. R. Dubois, "Adaptive Energy Management System Based on a Real-Time Model Predictive Control With Nonuniform Sampling Time for Multiple Energy Storage Electric Vehicle," *IEEE Trans. Veh. Technol.*, vol. 66, no. 7, pp. 5520–5530, Jul. 2017, doi: 10.1109/TVT.2016.2638912.
[19] J. P. Torreglosa, P. Garcia, L. M. Fernandez, and F. Jurado, "Predictive Control for the Energy Management of a Fuel-Cell–Battery–Supercapacitor Tramway," *IEEE Trans. Ind. Inform.*, vol. 10, no. 1, pp. 276–285, Feb. 2014, doi: 10.1109/TII.2013.2245140.
[20] K. Dalila, M. Abdessalem, D. Said, and L. Chrifi-Alaoui, "Robust linear parameter varying induction motor control with polytopic models," Serbian J. Electr. Eng., vol. 10, no. 2, pp. 335–348, 2013, doi: 10.2298/SJEE121218008D.

Mehdi Sellali received the M.S. degree in Renewable Energy from University of Biskra, Algeria, in 2016. He is currently working toward the Ph.D. degree with the Department of Electrical Engineering at the same university. He is an invited researcher in the Laboratory of Fuel Cell at the University of Technology of Belfort-Montbéliard (UTBM). His current research areas include modeling and energy management of hybrid energy storage systems, Hybrid Fuel Cell vehicles, and Electric vehicles. He developed activities in Automotive Systems Engineering, Electrical Engineering and Control Systems Engineering.

Achour Betka: was born in Biskra (Algeria) on March, 28th, 1969. On June, 1991, he obtained his graduate diploma of Applied university studies (DEUA), from Biskra University. On June, 1994, he got his engineering diploma in Electrical Engineering from Biskra University. On January 1998, holder of the Magister diploma in Elect. Eng. from the same university. From 1998 to 2004, he worked as assistant professor at Electrical Engineering department from the University of Oum El Bouaghi (Algeria), where he gave lectures on several Elect. Engin. subjects. He also taught Magister candidates on Electrical machines control. On December, 2010, holder of his PHD diploma from Batna University (Algeria). Till now, he works as a Professor at the Electrical Engineering department, Biskra University, and he is also, the Chief of the Renewable energy team at LGEB laboratory (www.lgeb.org), where he supervises several doctorate projects of different renewable energy topics. His research field includes Grid connected of renewable energy systems (photovoltaic, wind), and control of stationary hybrid systems .

Abdesslem Djerdir was born in 05/08/1969 and has received the B.S. degree in electrical engineering from the National Institute of Electrical Engineering Bejaia, Algeria, in 1993 and the Ph.D. degree in electrical engineering from University of Franche Comté Belfort, France, in 1999. Currently, he is a Full Professor at University of Technology Belfort-Montbéliard (UTBM), France. His research interests include modelling and design of electric and fuel cell vehicle systems (electrical machines, energy storage devices, and power converters). He develops his main researches on availability and high efficiency of electric drive trains for transport applications by combining the experimental and theoretical approaches. In this framework, he was the vehicle referent of the Mobypost project (http://mobypost-project.eu) where 10 fuel cell electrical vehicles were built and tested. Since December 2014 he is the head of the Energy department of UTBM.

Yongheng Yang (SM'17) received the B.Eng. degree in electrical engineering and automation from Northwestern Polytechnical University, Shaanxi, China, in 2009 and the Ph.D. degree in electrical engineering from Aalborg University, Aalborg, Denmark, in 2014. He was a postgraduate student with Southeast University, China, from 2009 to 2011. In 2013, he spent three months as a Visiting Scholar at Texas A&M University, USA. Currently, he is an Associate Professor with the Department

of Energy Technology, Aalborg University, where he also serves as the Vice Program Leader for the research program on photovoltaic systems. His current research is on the integration of grid-friendly photovoltaic systems with an emphasis on the power electronics converter design, control, and reliability. Dr. Yang is the Chair of the IEEE Denmark Section. He serves as an Associate Editor for several prestigious journals, including the IEEE TRANSACTIONS ON INDUSTRIAL ELECTRONICS, the IEEE TRANSACTIONS ON POWER ELECTRONICS, and the IEEE Industry Applications Society (IAS) Publications. He is a Subject Editor of the IET Renewable Power Generation for Solar Photovoltaic Systems. He was the recipient of the 2018 IET Renewable Power Generation Premium Award and was an Outstanding Reviewer for the IEEE TRANSACTIONS ON POWER ELECTRONICS in 2018.

Imen Bahri (M'13) was born in Tunisia in 1982. She received the Ing. and M.S degrees in electrical engineering from the National School Engineers of Tunis (ENIT), Tunis, Tunisia, in 2006 and 2007, respectively, and the Ph.D. degree from Cergy-Pon- toise University, Cergy-Pontoise, France, in 2011. She is currently an Assistant Professor with Paris-XI University, Orsay, France, and a member of the LGEP laboratory. Her current research in- terests include the control applications applied to automotive domain, the SoPC-based controllers, FPGA-based implementation of controllers, hardware/software (Hw/Sw) partitioning, and Hw/Sw codesign methodologies.

Saïd Drid (SM'13) was born in Batna, Algeria, in 1969. He received B.Sc., M.Sc. and PhD degrees in Electrical Engineering, from the University of Batna, Algeria, respectively in 1994, 2000 and 2005 respectively. He is Currently a full Professor at the Electrical Engineering Institute at University of Batna, Algeria. He is the head of the Energy Saving and Renewable Energy Team in the Research Laboratory of Electromagnetic Induction and Propulsion Systems of Batna University. In 2015, he spent two months as a Visiting professor at Picardie Jules Verne University, France. His research interests include electric machines and drives, renewable energy. He is also a reviewer for several prestigious journals (IET, IEEE, etc.) Prof. Drid is the Vice Chair of the PES chapter and the Treasurer of the IEEE Algeria Section. He serves as an Associate Editor for some international journals.